Study the effect of Ni doping on structural, optical and electrical properties of $Zn_{1-x}Ni_xO$ thin films deposited by spray pyrolysis technique

C. Zaouche[a,*], L. Dahbi[b], S. Benramache[a], A. Harouache[c], Y. Derouiche[d], M. Kharroubi[d], H. A. Haslouk[e], M. A. A. Banalhag[f], H. M. Alkhojah[g]
[a]*Material Sciences Department, Faculty of Science, University of Biskra, 07000 Biskra, Algeria*
[b]*Teacher Education College of Setif, Messaoude Zeghar, Algeria*
[c]*Center for Scientific and Technical Analyzes (CRAPC)-PTAPC, Laghouat, Algeria*
[d]*Physico-Chemistry of Materials and Environment Laboratory, Ziane Achour University of Djelfa, BP 3117, Djelfa, Algeria*
[e]*Faculty of sciences, University Sabratha, Libya*
[f]*Faculty of Public Health - Aljameel, University Sabratha, Libya*
[g]*Plant Department, University Sabratha, Libya*

The effect of Ni doping on structural, optical and electrical properties of deposited $Zn_{1-x}Ni_xO$ thin films on glass substrate by spray pyrolysis technique has been studied. The main objective of this research is to study the change of the physical and optical properties of $Zn_{1-x}Ni_xO$ thin films that are fabricant to semiconductor with different doping levels x. These levels are 0 at.%, 2 at.%, 4 at.%, 8 at.% and 12 at.%. The transmission spectra show that the $Zn_{1-x}Ni_xO$ thin films have a good optical transparency in the visible region from 88 to 95%. The optical gap energy of the $Zn_{1-x}Ni_xO$ thin films varied between 3.25 and 3.35 eV. The urbach energy varied between 65 and 230 meV. However, the $Zn_{0.88}Ni_{0.12}O$ thin films have many defects with maximum value of urbach energy. The $Zn_{0.88}Ni_{0.12}O$ thin films have minimum value of optical gap energy. The $Zn_{0.88}Ni_{0.12}O$ thin films have maximum value of the electrical conductivity which is 9.40 $(\Omega.cm)^{-1}$. The average electrical conductivity of our films is about (7.52 $(\Omega.cm)^{-1}$). XRD patterns of the $Zn_{1-x}Ni_xO$ thin films indicate that films are polycrystalline with hexagonal wurtzite structure.

(Received December 29, 2022; Accepted March 13, 2023)

Keywords: Zinc oxide, Thin films, Spray pyrolysis technique, Doping

1. Introduction

Researchers have given too much importance to transparent conductive oxides (TCOs) recently as they play a significant role in many different application areas such as ultraviolet lightemitting diodes (UV-LEDs) [1], transparent field-effect transistor (FETs), spintronic devices, photovoltaic solar cells (PVSC) [2], piezo- electric sensors [3], transparent electrodes [4] and optoelectronic components [5–7]. ZnO is a transparent semiconductor with wide band gap of 3.37 eV and large exciton binding energy of 60 meV [8–10]. TCO films, such as ZnO, are widely used as electrode layers in thin film solar cells, as they have a high degree of transparency in the visible wavelength range and high conductivity. Indium tin oxide (ITO) is an important TCO material that is greatly used today. However, it is possible that this material is somehow expensive and they may not keep it as an alternative product in the future. ITO may fail to respond to existing technology with production at a limited level. The product has high toxicity. So, the research for alternative results is needed. ZnO is regarded as an alternative to ITO due to its environmentally friendly and excellent optical and electrical properties. These properties of ZnO can be further improved by ion addition. In a study by Peng et al. [11] they found that pure ZnO thin films

*Corresponding author: zaouchechouaieb@gmail.com
https://doi.org/10.15251/JOR.2023.192.197

enhanced optical and electrical properties with indium doping at different ratios. With 0.5 at.% indium doping, the highest efficiency was achieved in terms of these properties. In another study, Madhi et al. [12] examined the optical and electrical properties of calcium-doped ZnO thin films and found that the transmittance of ZnO: Ca films was above 80% and the lowest electrical resistivity was about (5.10^{-3} Ω.cm) [13]. Sung et al. [14], studied Zr doped ZnO thin films grown on quartz substrates by RF sputtering technique and investigated the effect of Zr doping on the optical properties of ZnO. It was found that the optical transparency of the thin films was above 90%, but the optical band gap of the Zr doped ZNO (ZZO) thin films increased with Zr addition.

Different techniques such as magnetron sputtering [15], chemical vapor deposition (CVD) [16], pulsed laser deposition (PLD) [17] and sol gel processes [18] have been used to get ZnO thin films [19, 20]. Spray pyrolysis method is one of these techniques. It has different potential advantages than other techniques because of its lower crystallization temperature, low cost, simple deposition procedure, easier compositional control, and large surface area coating capability [21].

In this work, we have prepared Ni doped ZnO thin films by using the spray pyrolysis technique deposition on glass substrate which its temperature is 450 °C. We sprayed this glass substrate for 7 minutes. Ni doped ZnO thin films were synthesized with different doping levels (0, 2, 4, 8 and 12 at. %) for $Zn_{1-x}Ni_xO$. The $Zn_{1-x}Ni_xO$ thin films were used to enhance the optical and electrical properties of deposited thin films. However, we have studied the change of the optical, structural and electrical properties of $Zn_{1-x}Ni_xO$ thin films that are fabricant to semiconductor.

2. Experimental procedure

$Zn_{1-x}Ni_xO$ solutions were prepared by dissolving the zinc acetate ($Zn(CH_3.CO_2)_2.2H_2O$) and nickel acetate ($Ni(CH_3.CO_2)_2.4H_2O$) with 0.5 mol l^{-1}. In this work, we have used a Ni doping with different concentrations in the game Ni/Zn = 0, 2, 4, 8 and 12 at. % or (x = 0, 0.02, 0.04, 0.08 and 0.12). Then we have added a drop of HCl for the sake of stabilizing heating solution. We agitated and heated the mixture solution at 50 °C for 3 h to prepare a clear and transparent solution. After 24 h, we sprayed the glass substrate.

The $Zn_{1-x}Ni_xO$ samples were prepared by spraying the solution onto glass substrate where its temperature was 450 °C. It took 7 minutes to obtain a thin film. The $Zn_{1-x}Ni_xO$ thin films were prepared at different Ni doping levels which are 0 at.%, 2 at.%, 4 at.%, 8 at.% and 12 at.%. After the deposition of the thin films, we let the substrate so that its temperature would decrease and be similar to the one of the room.

The structural properties of $Ni_{1-x}Zn_xO$ thin films were studied by means of X-ray diffraction (XRD Bruker AXS-8D) with CuKa radiation (λ=0.15406 nm) in the scanning range of (1h) which was between 20° and 70°. The optical transmission of the deposited films was measured in the range of (300–900nm) by using an ultraviolet-visible spectrophotometer (LAMBDA 25) and the electrical conductivityσ was measured by four point methods.

3. Results and discussion

3.1. Structural properties of $Zn_{1-x}Ni_xO$ thin films

The crystal structure of the pure ZnO and Ni doped ZnO was analyzed by X-Ray Diffraction (XRD) method. The obtained XRD patterns of the pure ZnO and Nickel doped ZnO thin films were shown in Figure 1. Figure 1 shows that the XRD peaks at 31.8721°, 34.5588°, 36.3220° and 56.7670° corresponding to (100), (002), (101), and (110) crystal planes, respectively. For all thin films, XRD results (Ref. JCPDS-Card No. 36-1451) showed that it was hexagonal wurtzite structure which has a preferential c-axis orientation [11, 12, 22, 23]. Figure 1 shows that the Ni doping level has a critical role in improving the crystallinity of ZnO thin films. It can be said that the crystallinity of $Zn_{1-x}Ni_xO$ films with 0.12 at.% Ni is better than that of other films. A similar result was found by Gupta et al. [24, 25], for indium-doped ZnO where thin films prepared by the PLD technique. Gupta et al. also noted that much higher indium doping destroyed the crystallinity of ZnO thin films. As a result, the rate of Ni doping has played a vital role in the

crystallization of ZnO thin films. Also we see the decrease of intensity of the (002) peak with the increase of the doping level x at 0.12. As it can be seen in Table 1, the position of (002) peak shifts slightly to lower angle. In our study, Ni atoms added to pure ZnO lattice structure create crystal stress or defect within the structure. Crystal defects and stresses are thought to cause significant change in crystal structure. In the XRD spectra, the broadening, narrowing or more intensity of the peaks can be estimated to the crystal structure defects formed by the addition of Ni atoms (see Table 1).

The stress ε_{zz}, was estimated using the following formula [26].

$$\varepsilon_{zz} = \frac{c - c_0}{c_0} * 100 \tag{1}$$

The lattice constant c of ZnO thin films and c_0 the lattice constant of bulk (standard c_0=0,5206nm).

The average crystallite size G for the (002) plane of thin films was calculated using the Debye–Scherrer equation [27].

$$G = \frac{0.9\lambda}{\beta \cos\theta} \tag{2}$$

where$G$ is the crystallite size, $\beta$is the full width at half-maximum (FWHM), $\theta$is Bragg angle of the diffraction peaks and $\lambda$is the X-ray wavelength (λ=0.15406 nm). The variations are shown in Table 1. In Table 1, we observed the decrease of G from 30.21592 to 21.1471nm with the increase of doping level x from x=0.02 to x=0.12, while it was 105.7504nm for the pure ZnO thin film.

Secondly, the dislocation density (δ_{hkl}), which measures the amount of defects in a crystal, is defined by the length of dislocation lines per unit volume. We used the following formula in order to determine it [28, 29].

$$\delta_{\mathrm{hkl}} = \frac{1}{G^2} \tag{3}$$

In Table 1, also we observed that the $Zn_{0.88}Ni_{0.12}O$ thin films have maximum value of the dislocation density (δ_{hkl}).

We used Bragg's law so that we can determine the interplanar distance d and this law is given as follows [30].

$$n\lambda = 2d \sin\theta \tag{4}$$

where n is an integer (n = 1) and θ corresponds to the half-diffraction angle. The distance d of each film for (002) plane is given in Table 1. Table 1 data is in good agreement with standard data (JCPDS No. 36-1451).

In addition, the lattice constant (c) of the thin films was calculated from the XRD data presented in Table 1 using the following equation [31].

$$\frac{1}{\mathrm{d}_{\mathrm{hkl}}^2} = \frac{4}{3}\frac{\mathrm{h}^2 + \mathrm{k}^2 + \mathrm{hk}}{\mathrm{a}^2} + \frac{\mathrm{l}^2}{\mathrm{c}^2} \tag{5}$$

The calculated value of the lattice constant (c) for the pure ZnO thin film is 0.519597nm. Depending on the increase of Ni doping rate, the value reached 0.518989 nm at doping level x=0.12. These calculated values for thin films agree well with standard data (JCPDS No. 36-1451, c_0 = 0.5206 nm).

The variations of the crystallite size and diffraction angle according to (002) peak are presented in Figure 2. It shows the variation of crystallite size and diffraction angle of Zn doped NiO thin films as a function of Zn doping level. Figure 2 shows that the diffraction angles of (002)

plan increased then decreased with the increase of doping levels x to reach the minimum value which was obtained at x=0.12 for $Zn_{0.88}Ni_{0.12}O$ thin films (see Table 1). We observed the decrease of the crystallite size of (002) plan to minimum value at x=0.12. The decrease of the crystallite size proves the enhancement of the crystallinity of Ni doped ZnO thin films. it can be said that This result explain the coalescence of the crystallite of the thin films to improve with oxygen diffusion [32].

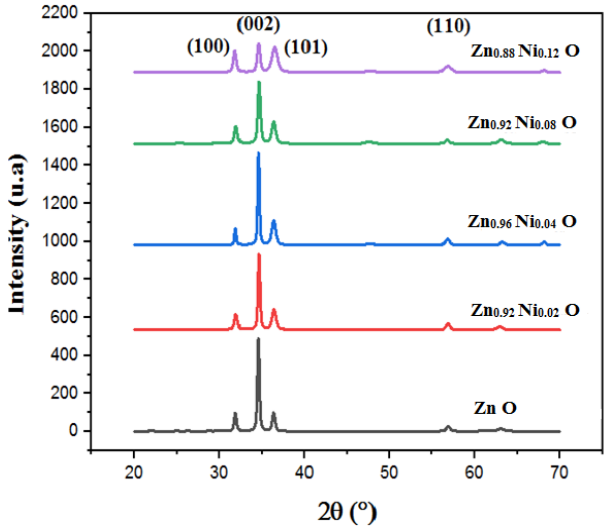

Fig. 1. X-ray diffraction of $Zn_{1-x}Ni_xO$ thin films as a function of Ni doping level.

Table 1. The structural parameters of $Zn_{1-x}Ni_xO$ thin film as a function of Zn doping level of (002) diffraction peak.

X	2θ(°)	d (nm)	G (nm)	$\beta_{1/2}$ (°)	ε_{zz} (%)	δ (m^{-2})	C (nm)
0	34,5124	0,259798	105,7504	0,0787	-0.19269	$8,94202*10^{13}$	0,519597
0.02	34,5978	0,259177	30,21592	0,2755	-0.43156	$1,1*10^{15}$	0,518353
0.04	34,5638	0,259424	60,40433	0,1378	-0.3366	$2,74*10^{14}$	0,518848
0.08	34,566	0,259408	60,40469	0,1378	-0.34275	$2,74*10^{14}$	0,518816
0.12	34,5541	0,259494	21,1471	0,3936	-0.30948	$2,24*10^{15}$	0,518989

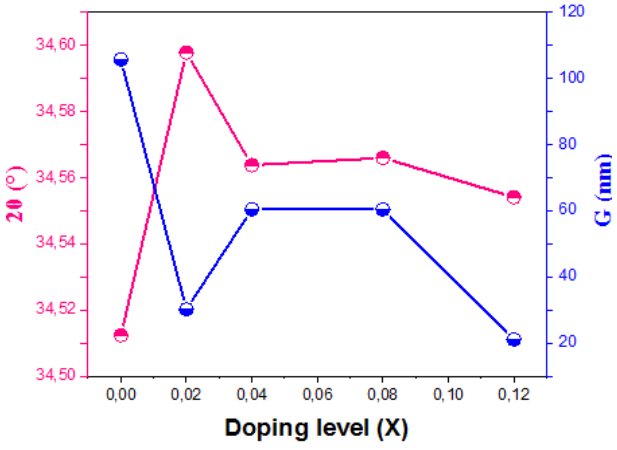

Fig. 2. The variation of crystallite size and diffraction angle of Ni doped ZnO thin films according to(002) phase

3.2. Optical properties of $Zn_{1-x}Ni_xO$ thin films

The Optical characterizations of fabricated $Zn_{1-x}Ni_xO$ thin films by doping levels x were performed by measuring the transmittance and absorbance in the wavelength region 300 to 900 nm as it is shown in Figure 3. As we can see, the value of the average transmission of spray $Zn_{1-x}Ni_xO$ thin films is about 92% in the visible region. But for these doping levels x, the region of the absorption edge was located between 361 and 379 nm in comparison with others which are found at 355 and 370 nm [33]. It is related region between of the valence band and the conduction band. The inset of Figure 3 presents the variation of absorbance data of thin films of $Zn_{1-x}Ni_xO$. The absorption edge shifts was observed clearly at wavelength shorter than 390nm. The absorption edge shifts of $Zn_{1-x}Ni_xO$ thin films increased with the increase of doping levels x. As we can note, the optical property of thin films of $Zn_{1-x}Ni_xO$ is affected by doping levels x.

The role of doping levels x on the transmission of thin films of $Zn_{1-x}Ni_xO$ was clearly observed on the thin films quality due to the higher transparency. The high transparency was obtained in Ni doped ZnO thin film with at 2% due to the interstitial site of Zn and Ni. That absorbance and the optical band gap energy E_g of fabricated $Zn_{1-x}Ni_xO$ thin films were determined by the following relations [34– 35]:

$$A = \alpha d = -\ln T \tag{6}$$

$$(Ahv)^2 = C(hv - E_g) \tag{7}$$

where A is the absorbance of fabricated $Zn_{1-x}Ni_xO$ thin films, α is the absorption coefficient, d is the film thickness, T is the transmission of fabricated $Zn_{1-x}Ni_xO$ thin films, C is a constant, hυ is the energy of photon ($h\upsilon = \frac{1240}{\lambda(\text{nm})}$ (eV)) and E_g is the band gap energy of the semiconductor. However, the disorder or Urbach energy (E_u) also was determined by the expression follow [36–37]:

$$A = A_0 \exp\left(\frac{hv}{E_u}\right) \tag{8}$$

where A_0 is a constant, hυ is the energy of photon and E_u is the Urach energy, the tail width of the Urbach energy was used to characterize the order of the defects. The variation of optical band gap energy and Urbach energy of fabricated $Zn_{1-x}Ni_xO$ thin films as a function of doping levels x are presented in the Figure 4. The band gap energy was observed a smaller than 3.36 eV. The value of band gap energy decreased with the increase in doping levels from 3.35 to 3.25 eV. The diminution in the optical band gap energy value of $Zn_{1-x}Ni_xO$ thin films can be illustrated by the effect of quantum confinement due to the diminution in the crystallite size of fabricated $Zn_{1-x}Ni_xO$ thin films (see Figure 2).

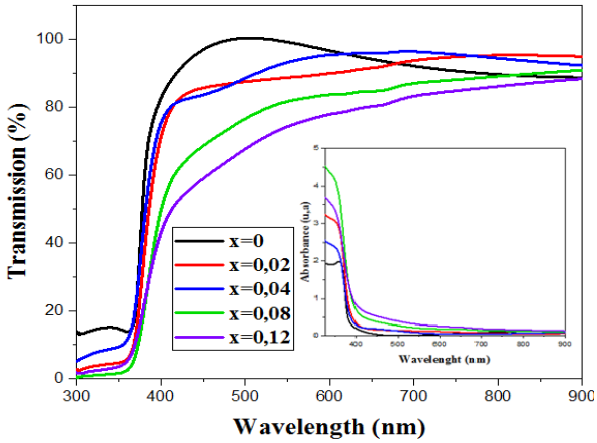

Fig. 3. Transmission spectra of $Zn_{1-x}Ni_xO$ thin films as a function of Ni doping level.

As can be seen in Figure 4 that the value of Urbach energy increased with the increase in doping levels from 65 to 230 meV. Also, this can be related by the diminution of the crystallite size value (see Figure 2).

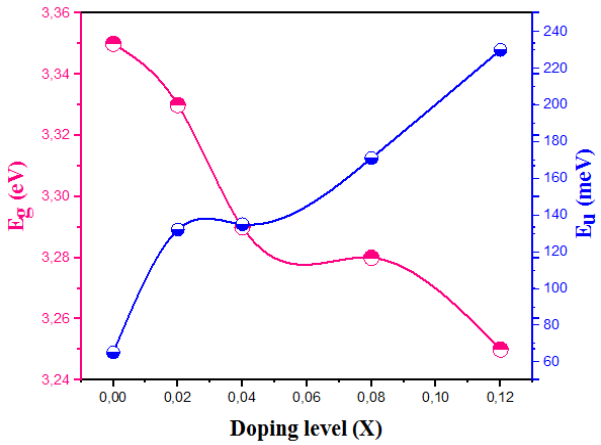

Fig. 4. The variations of optical pand gap energy and Urbach energy of Ni doped ZnO thin films at various doping levels

3.3. Electrical properties of $Zn_{1-x}Ni_xO$ thin films

The four-points probe method was used to determine the electrical conductivity of $Zn_{1-x}Ni_xO$ thin films, it is based on measuring the sheet resistance of the films as expressed by:

$$R_{sh} = \frac{\pi}{\ln(2)} \cdot \frac{V}{I} \tag{9}$$

where I is the applied currant = 1 nA and V is the measurement voltage. However, the electrical conductivity σalso is determined by the following equation:

$$\sigma = \frac{1}{d.R_{sh}} \tag{10}$$

Figure 5 shows the variation of the electrical conductivity of Ni doped ZnO thin films as a function of Ni doping level. As can be seen, the electrical conductivity increases with increasing the Zn doping level up to 12 at.% where we obtained a maximum conductivity value which was $9.40(\Omega.cm)^{-1}$. The increase in the conductivity of the $Ni_{1-x}Zn_xO$ thin films can be explained by the displacement of the electrons. The latter comes from the Ni^{+2} donor ions in the substitutional sites of Zn^{+2} and the formation of the molecular ZnNiO existed on the surface. The Figures (2, 4 and 5) showed the decrease in the crystallite size, the decrease in optical gab energy, the increase in urbach energy and the increase in electrical conductivity. These results explain the good crystallization of the thin films according to [38– 39– 40– 41].

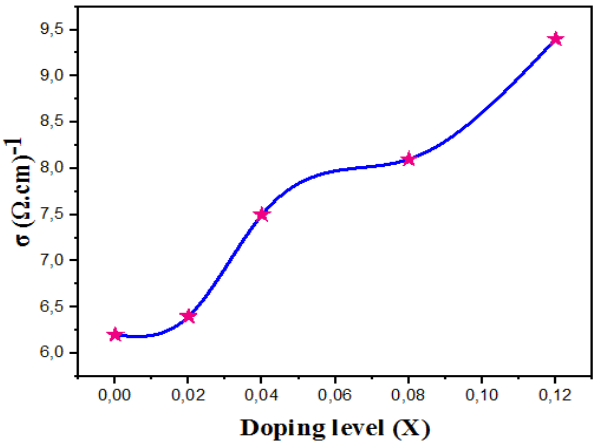

Fig. 5. The electrical conductivity variation of $Zn_{1-x}Ni_xO$ thin films as a function of Ni doping level.

4. Conclusion

In this study, Nickel doped Zinc Oxide thin films (Ni/Zn = 0, 2, 4, 8 and 12 at.%) were successfully deposited on glass substrate by spray pyrolysis technique using Nickel acetate and Zinc acetate. The $Zn_{1-x}Ni_x$Othin films are transparent in the visible region. The variation of the optical gap energy is between 3.25 and 3.35 eV. The variation of the Urbach energy is between 65 and 230 meV. However, the $Zn_{0.88}Ni_{0.12}$Othin films have many defects with maximum value of urbach energy.

The $Zn_{0.88}Ni_{0.12}$Othin films have minimum value of optical gap energy. Also, the $Zn_{0.88}Ni_{0.12}$Othin films have maximum value of the electrical conductivity and have minimum value of the crystallite size which is 21.1471nm. XRD patterns of the $Zn_{1-x}Ni_x$Othin films indicate that films are polycrystalline with hexagonal wurtzite structure. The electrical conductivity of deposited films is in the order of 7.52$(\Omega.cm)^{-1}$. The Figures (2, 4 and 5) shows the decrease in the crystallite size, the decrease in optical gab energy, the increase in urbach energy and the increase in electrical conductivity. These results explain the good crystallization of the thin films.

References

[1] J. Song, Y. He, J. Chen, D. Zhu, Z. Pan, Y. Zhang, J. Wang, Journal of ElectronicMaterials 41, 431(2012) ; https://doi.org/10.1007/s11664-011-1783-x

[2] J. Huang, Z. Yin, Q. Zheng, EnergyEnvironmental Science 4, 3861(2011) ; https://doi.org/10.1039/c1ee01873f

[3] T. Xu, G. Wu, G. Zhang, Y. Hao, Sensors and Actuators A Phys3ical 104, 61(200) ; https://doi.org/10.1016/S0924-4247(02)00484-3

[4] G. A. Hirata, J. McKittrick, T. Cheeks, J. M. Siqueiros, J. A. Diaz, O. Contreras, O. A. Lopez,Thinsolid films 288, 29(1996) ; https://doi.org/10.1016/S0040-6090(96)08862-1

[5] B. Nasr, S. Dasgupta, D. Wang, N. Mechau, R. Kruk, H. Hahn, Journal of AppliedPhysics 108, 103721(2010) ; https://doi.org/10.1063/1.3511346

[6] Z. A. Wang, J. B. Chu, H. B. Zhu, Z. Sun, Y. W. Chen, S. M. Huang, Solid-State Electron 53, 1149(2009) ; https://doi.org/10.1016/j.sse.2009.07.006

[7] W. Beyer, J. Hüpkes, H. Stiebig, Thin Solid Films 516, 147(2007) ; https://doi.org/10.1016/j.tsf.2007.08.110

[8] L. E. Greene, M. Law, D. H. Tan, M. Montano, J. Goldberger, G. Somorjai, P. Yang, Nano Letters 5, 1231(2005) ; https://doi.org/10.1021/nl050788p

[9] C. Huang, M. Wang, Z. Deng, Y. Cao, Q. Liu, Z. Huang, Y. Liu, W. Guo, Q. Huang,

Semiconductor Science and Technology 25, 045008(2010) ; https://doi.org/10.1088/0268-1242/25/4/045008
[10] C. Klingshirn, PhysicaStatusSolidi B 71, 547(1975) ; https://doi.org/10.1002/pssb.2220710216
[11] L. Peng, L. Fang, Y. Zhao, W. Wu, H. Ruan, C. Kong, Journal of Wuhan University of Technology. Mater. Sci. Ed 32, 866(2017) ; https://doi.org/10.1007/s11595-017-1681-z
[12] H. Mahdhi, Z. B. Ayadi, J. L. Gauffier, K. Djessas, S. Alaya, Optical Materials 45, 97(2015) ; https://doi.org/10.1016/j.optmat.2015.03.015
[13] H. Mahdhi, K. Djessas, Z. B. Ayadi, MaterialsLetters 214, 10(2018) ; https://doi.org/10.1016/j.matlet.2017.11.108
[14] N. E. Sung, K. S. Lee, I. J. Lee,Thin Solid Films 651, 42(2018) ; https://doi.org/10.1016/j.tsf.2018.02.011
[15] X. Jiang, F. L. Wong, M. K. Fung, S. T. Lee, AppliedPhysicsLetters 83, 1875(2003) ; https://doi.org/10.1063/1.1605805
[16] I. Volintiru, M. Creatore, B. J. Kniknie, Journal of AppliedPhysics 102, 043709(2007) ; https://doi.org/10.1063/1.2772569
[17] Y. Liu, L. Zhao, J. Lian, Vacuum 81, 18(2006) ; https://doi.org/10.1016/j.vacuum.2006.02.001
[18] Y. Caglar, M. Caglar, S. Ilican, A. Ates, Journal of Physics D. AppliedPhysics 42, 065421(2009) ; https://doi.org/10.1088/0022-3727/42/6/065421
[19] B. Singh, Z. A. Khan, I. Khan, S. Ghosh, AppliedPhysicsLetters 97, 241903(2010) ; https://doi.org/10.1063/1.3525575
[20] M. Y. Zhang, G. J. Cheng, AppliedPhysicsLetters 99, 051904(2011) ; https://doi.org/10.1063/1.3622645
[21] C. Zaouche, Y. Aoun, S. Benramache, A. Gahtar, Scientific Bulletin of valahiaUniversitymaterials and mechanics 17(17), 27(2019) ; https://doi.org/10.2478/bsmm-2019-0015
[22] G. K. Paul, S. Bandyopadhyay, S. Sen, MaterialsChemistry and Physics 79, 71(2003) ; https://doi.org/10.1016/S0254-0584(02)00454-6
[23] G. Malik, J. Jaiswal, S. Mourya, R. Chandr, Journal of AppliedPhysics 122, 143105(2017) ; https://doi.org/10.1063/1.5007717
[24] R. K. Gupta, K. Ghosh, R. Patel, S. R. Mishra, P. K. Kahol. Journal of Crystal Growth 310, 3019(2008) ; https://doi.org/10.1016/j.jcrysgro.2008.03.004
[25] S. Mondal, P. Mitra, Indian Journal of Physics 87, 125(2013) ; https://doi.org/10.1007/s12648-012-0198-8
[26] A. J. Hashim, M. S. Jaafar, A. J. Ghazai, N. M. Ahmed, Optik 124, 491(2013) ; https://doi.org/10.1016/j.ijleo.2011.12.059
[27] S. Benramache, S. Gareh, B. Benhaoua, A. Darsouni, Journal of Chemistry and MaterialsResearch 2, 59(2015).
[28] V. P. Patil, S. Pawar, M. Chougule, P. Godse, R. Sakhare, S. Sen, P. Joshi, Journal of Surface EngineeredMaterials and Advanced Technology 01, 35(2011) ; https://doi.org/10.4236/jsemat.2011.12006
[29] V. Kumar, D. k. Sharma, K. Sharma, D. k. Dwivedi, Optik 156, 43(2018) ; https://doi.org/10.1016/j.ijleo.2017.10.169
[30] R. J. Tilley, Crystals and Crystal Structures (Wiley, New York, 2006).
[31] E. F. Keskenler, G. Turgut, S. Doğan, Superlattices and Microstructures 52, 107(2012) ; https://doi.org/10.1016/j.spmi.2012.04.002
[32] S. Benramache, B. Benhaoua, Superlattices and Microstructures 52, 1062(2012) ; https://doi.org/10.1016/j.spmi.2012.08.006
[33] O. Bayram, E. Sener, E. İgman. O. Simsek, Journal of Materials Science Materials in Electronics 30, 3452(2019) ; https://doi.org/10.1007/s10854-018-00620-2

[34] A. Diha, S. Benramache, B.Benhaoua, Optik 172, 832(2018) ; https://doi.org/10.1016/j.ijleo.2018.07.062

[35] S. Benramache, Y. Aoun, S. Lakel, H. Mourghade, R. Gacem, B. Benhaoua, Journal of Nano- and ElectronicPhysics 10, 06032(2018) ; https://doi.org/10.21272/jnep.10(6).06032

[36] W. Daranfed, M. S. Aida, A. Hafdallah, H. Lekiket, Thin Solid Films 518, 1082(2009) ; https://doi.org/10.1016/j.tsf.2009.03.227

[37] A. Gahtar, S. Benramache, C. Zaouche, A. Boukacham, A. Sayah, Advances in Materials Science 20(3), 36(2020) ; https://doi.org/10.2478/adms-2020-0015

[38] C. Zaouche, A. Gahtar, S. Benramache, Y. Derouiche, M. Kharroubi, A. Belbel, C. Maghni, L. Dahbi, Digest Journal of Nanomaterials and Biostructures 17(4), 1453(2022) ; https://doi.org/10.15251/DJNB.2022.174.1453

[39] S. Benramache, Y. Aoun, A. Charef, B. Benhaoua, S. Lake, Inorganic and Nano-MetalChemistry 49, 177(2019) ; https://doi.org/10.1080/24701556.2019.1624568

[40] M. Othmane, A. Attaf, H. Saidi, F. Bouaichi, N. Lehraki, M. Nouadji, M. Poulain, S. Benramache, International Journal of Nanoscience 15, 1650007(2015) ; https://doi.org/10.1142/S0219581X16500071

[41] A. Gahtar, A. Benali, S. Benramache, C. Zaouche, ChalcogenideLetters 19(2), 103(2022) ; https://doi.org/10.15251/CL.2022.192.103